

This article was downloaded by:

On: 15 January 2011

Access details: *Access Details: Free Access*

Publisher *Taylor & Francis*

Informa Ltd Registered in England and Wales Registered Number: 1072954 Registered office: Mortimer House, 37-41 Mortimer Street, London W1T 3JH, UK



Comments on Inorganic Chemistry

Publication details, including instructions for authors and subscription information:

<http://www.informaworld.com/smpp/title~content=t713455155>

Magnetism and Structure: Model Studies on Transition Metal Fluorides and Cyanides

D. Babel^a

^a Fachbereich Chemie und Sonderforschungsbereich 127 ("Kristallstruktur und Chemische Bindung") der Philipps-Universität, Marburg, Federal Republic of Germany

To cite this Article Babel, D.(1986) 'Magnetism and Structure: Model Studies on Transition Metal Fluorides and Cyanides', *Comments on Inorganic Chemistry*, 5: 6, 285 – 320

To link to this Article: DOI: 10.1080/02603598608081849

URL: <http://dx.doi.org/10.1080/02603598608081849>

PLEASE SCROLL DOWN FOR ARTICLE

Full terms and conditions of use: <http://www.informaworld.com/terms-and-conditions-of-access.pdf>

This article may be used for research, teaching and private study purposes. Any substantial or systematic reproduction, re-distribution, re-selling, loan or sub-licensing, systematic supply or distribution in any form to anyone is expressly forbidden.

The publisher does not give any warranty express or implied or make any representation that the contents will be complete or accurate or up to date. The accuracy of any instructions, formulae and drug doses should be independently verified with primary sources. The publisher shall not be liable for any loss, actions, claims, proceedings, demand or costs or damages whatsoever or howsoever caused arising directly or indirectly in connection with or arising out of the use of this material.

Magnetism and Structure: Model Studies on Transition Metal Fluorides and Cyanides

Magnetochemical studies performed on 3d transition metal fluorides and cyanides are reported. The antiferromagnetic and ferrimagnetic behavior observed for various members of the two series of compounds is shown to depend on the geometric and electronic features of the crystal structures and ions. Variation of these features for selected model substances has permitted the separation of the different influences, and these are systematically discussed by using simple qualitative aspects of chemical bonding.

I. INTRODUCTION

Magnetic measurements provide a classical tool to obtain bonding and structural information on transition metal compounds.¹⁻⁷ However, the magnetic properties of compounds are not merely determined by the transition metal ion and its first coordination sphere. In addition to the local ligand field acting on the partly filled electron shell of a central cation, magnetic interactions between different paramagnetic centers may also be important. In the case of molecular compounds the number of interacting centers is limited, e.g., in di- and polynuclear complexes, or, especially, in cluster compounds. The presence of direct metal-metal bonding in compounds like these is frequently detected by means of magnetic studies.

On the other hand, in extended ionic solids an unlimited number of centers may interact on a long-range scale, and these interactions

may give rise to cooperative phenomena such as ferro-, antiferro- and ferrimagnetism. These important nonmolecular magnetic interactions are indicated by characteristic susceptibility and magnetization curves, and compounds of this class generally exhibit well-defined magnetic structures as well. The magnetic structures result from parallel, antiparallel or canted spin alignments, the patterns of which are detectable below the ordering temperatures by neutron diffraction techniques.

Antiferromagnetism is quite a usual property among magnetically nondilute transition metal ionic solids. It is nearly always claimed if the magnetic moment of a compound is reduced compared with the spin-only moment or whatever is considered "normal" for the ion in question. However, since other factors such as high spin-low spin transitions may also cause a reduction in the magnetic moment, care has to be taken in the interpretation of magnetic data. The observed magnetic properties may reflect several quite different influences.

In the course of our structural studies on transition metal fluorides^{8,9} we have also investigated the magnetic behavior of the compounds, and antiferromagnetism has often been indicated. The fluoride ion is an extremely ionic and weak-field ligand. Thus, other reasons for the observed reduction of magnetic moments in nearly undistorted, but infinitely linked octahedra, may be excluded. Therefore, keeping both the ligand and the coordination number constant, the variation of magnetism found may be assumed to reflect the influence of the structure of the compound and of the transition metal ion properties on magnetic interactions.

With this premise we will give a systematic account of data gathered on transition metal fluoride compounds over a period of many years.¹⁰⁻¹⁸ In the last section, the ideas developed in the discussions on the fluorides are extended to the other bonding extreme, namely, that occurring in a series of transition metal cyanide compounds which we have studied recently.¹⁹⁻²¹

Since there are excellent books and reviews on the theory and physics of magnetic interactions,²²⁻²⁷ it is the aim of this Comment to stay within the chemist's world and to interpret the experimental findings by applying only simple chemical concepts of structure and bonding. The important field of magnetic interactions in solids may be seen in this way to be less separated from the general interests of chemists.

II. THE SUPEREXCHANGE MODEL OF MAGNETIC INTERACTIONS

In the class of ionic compounds to be discussed, the magnetic cations generally do not approach one another sufficiently to make direct interactions possible between them. Rather an indirect mechanism, called "superexchange," acts via the anion bridges that connect the cations. The model, originally proposed by Kramers²⁸ and later applied by Anderson,²⁹ was summarized in qualitative rules by Goodenough^{2,30} and Kanamori.³¹ These rules are easy to understand. They require the assumption of a partial covalence between the ligand and its cation neighbors on both sides. Since the electrons in the overlapping p- and d-orbitals are subject to both the Pauli principle and to Hund's rule (of maximum spin at the transition metal ions), the consequences of relative cation spin orientations illustrated in Fig. 1 follow for the different cases of σ - and π -transfer. It may be anticipated that the π -mechanism, because of smaller overlap, generally makes a smaller contribution, especially in fluorides.

In a simplified picture which neglects the differentiation between correlation and delocalization effect in superexchange,² it is the antiparallelism of the two electrons within an anion orbital—one electron drawn on each side—that makes the cation spins antiparallel. Thus, antiparallel coupling is the result in both symmetric situations, where the overlap with the cations involves either empty or half-filled d-orbitals on both sides of the anion. However, the coupling is stronger in the latter case, since the electron concentration is higher in the affected orbitals and the driving force for the assumed mechanism is greater. Parallel, i.e., ferromagnetic, spin coupling via more or less linear bridges results only in the mixed case of unsymmetric overlap with empty d-orbitals on one side of the anion and half-filled ones on the other side.

The relative strength of σ and π coupling will change when the bridge angle changes. At right angles σ transfer along only one anion orbital vanishes, but at the same time a ferromagnetic 90° interaction involving two anion orbitals comes into play. This mechanism is important in chalcogenides and the heavier halides, but it is negligible in fluorides except at the lowest temperatures.

The model sketched here shows that superexchange interactions depend on factors of chemical relevance. These factors, which with

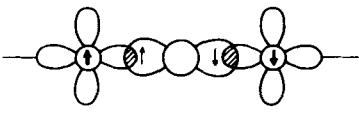
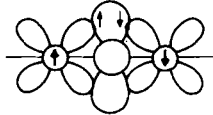
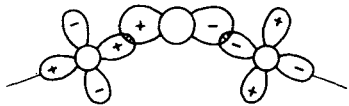
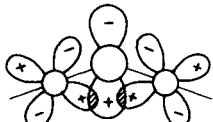
σ-Superexchange		π-Superexchange	
 $d_{x^2-y^2}$ p_x $d_{x^2-y^2}$		 d_{xy} p_y d_{xy}	
			
$d_{x^2-y^2}^0$	--- $d_{x^2-y^2}^0$	antiferro- magnetic	d_{xy}^0 --- d_{xy}^0
$d_{x^2-y^2}^1$	--- $d_{x^2-y^2}^1$		d_{xy}^1 --- d_{xy}^1
$d_{x^2-y^2}^0$	--- $d_{x^2-y^2}^1$	ferro- magnetic	d_{xy}^0 --- d_{xy}^1

FIGURE 1 σ - and π -superexchange via linear and bent anion bridges. The arrows drawn in the linear case designate spin orientations resulting from anion orbital overlap with empty d-orbitals. Other electronic configurations leading to antiferromagnetic and ferromagnetic coupling are noted.

fluorides mainly concern σ effects, will be experimentally examined in the subsequent sections by studying the following influences:

- (1) Structure and geometry: dimensionality, angle, and kind of linking octahedra.
- (2) Cation properties: charge, size, electron configuration, and bonding towards the anion.

III. EXPERIMENTAL ESTIMATES ON THE INTENSITY OF MAGNETIC INTERACTIONS

To determine separately the effect of the different influences just mentioned, it is necessary to select related compounds in which as many parameters as possible may be held constant and only one

parameter changed at a time. Therefore, to show the dependence of magnetic properties on geometric factors, different compounds will first be compared in which the transition metal ion is kept the same while the structure is varied. In this case the effective magnetic moment, $\mu_{\text{eff}} = 2.828\sqrt{\chi T}$, is a useful measure of the magnetism exhibited and of its departure from "normal" values. (χ is the experimental molar susceptibility, which in this Comment always refers to one mole content of paramagnetic ions). To display the temperature dependence, which in antiferromagnetic substances above the ordering point often follows a Curie-Weiss law ($\mu_{\text{CW}} = 2.828\sqrt{\chi(T - \theta)}$ or $\chi^{-1} = (T - \theta)/\mu_{\text{CW}}^2 = (T - \theta)/C$), it is common to plot the reciprocal susceptibility, χ^{-1} , vs. T . In general, the stronger the antiferromagnetic interactions are, the greater is the negative magnitude of θ and the higher the χ^{-1} curves lie. So the sequence of these curves reflects changes of magnetic interactions, and this sequence is sufficient to estimate the effect of the parameters identified above and their relative influence in isoelemental compounds. Therefore quantitative measures for the coupling strength, such as exchange energies, which are not so simple to evaluate and which vary up to a factor of 5 depending on the model,^{32,68} seem unnecessary for our qualitative purposes. However, another parameter which implies energy, the three-dimensional antiferromagnetic ordering or Néel temperature, may also be used. To a first approximation this value is given by the temperature at which a minimum occurs in the reciprocal susceptibility vs. temperature plots shown later. The Néel temperature T_N correlates with the coupling strength since it marks the point where the cooperative spin-ordering forces overcome thermal energy. In our compounds we will generally compare T_M , the temperature of minimum χ^{-1} , though in low-dimensional systems this minimum only indicates pre-ordering on a short-range scale.

The use of the estimates of the coupling strength becomes problematic in the comparison of compounds in which the magnetic cation is varied. This variation, which is treated in the second of the following sections, demonstrates the influence of cation properties on magnetic behavior. It requires not only constant geometry by choice of isostructural compounds, but also a normalization of the magnetic moments of the different cations so as to make them comparable. This is achieved in this work by expressing the observed effective moments μ_{eff} in units of some normal moments

μ_0 . For these normal values, the effective moment will be taken as the value that is experimentally found at the same temperature in a reference compound of the corresponding cation. The reference compound will be one in which the same ligands (and ligand-field parameters) are present, but in which the absence of magnetic interactions is assumed. This assumption, though not unarbitrary, should be valid to an acceptable approximation for transition metal fluorides that have structures in which the coordination octahedra are isolated.⁶⁷ Figure 2 shows the reciprocal susceptibility plots of some reference compounds selected here, and Table I lists the data

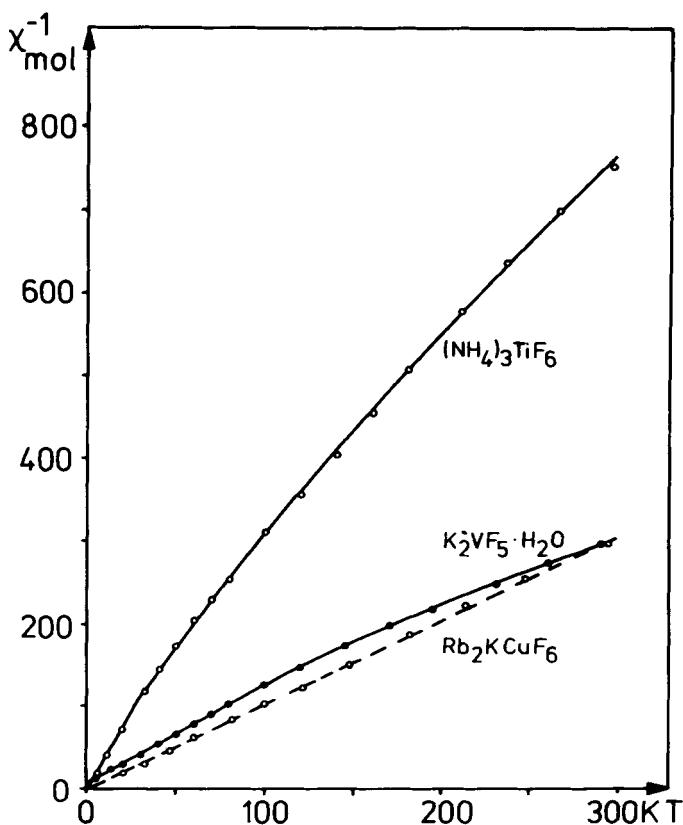


FIGURE 2 Reciprocal susceptibility plots of some fluorides used as "interaction-free" reference compounds.

TABLE I

Magnetic parameters of reference compounds assumed to exhibit no interactions. The reference magnetic moment μ_0 at temperature $T(K)$ is calculated from the Curie-Weiss parameters by $\mu_0 = \mu_{CW}(T/T - \theta)^{1/2}$. Larger and temperature dependent θ values indicate curvatures of the χ^{-1} vs. T plots (see Fig. 2), due to spin-orbit coupling (Refs. 3 and 7)

Electronic Configuration, Ion	Reference Compound	Temperature Range (K)	μ_{CW} (BM)	θ (K)	Shown in Fig.	Ref.
d ¹ Ti ³⁺	(NH ₄) ₃ TiF ₆	4–30 30–100 100–300	1.477 1.676 1.855	0 –11 –36	2	[16]
d ² V ³⁺	K ₂ VF ₅ ·H ₂ O	5–100 100–300	2.588 2.983	–6 –46	2	[16]
d ⁶ Co ³⁺	Cs ₂ KCoF ₆	<450	5.540	0		[16],[67]
d ⁷ Co ²⁺	CoF ₂ ·4H ₂ O	<320	5.197	–27		[11],[14]
d ⁸ Ni ²⁺	Li ₂ NiF ₄	<470	3.163	0	5	[10],[14]
d ⁸ Cu ³⁺	Rb ₂ KCuF ₆	<300	2.831	1	2	[16]
d ⁹ Cu ²⁺	Na ₂ CuF ₄	<470	1.980	–11	6	[11],[14]

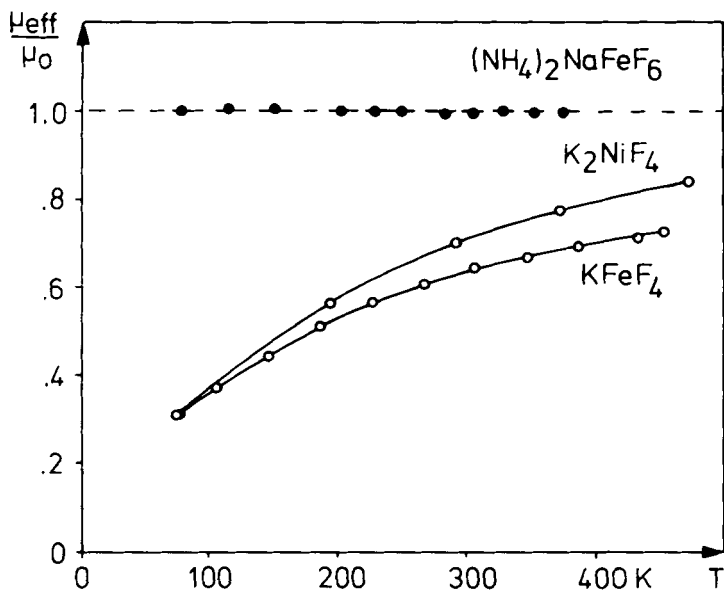


FIGURE 3 Normalization of effective magnetic moment by expressing it in units of μ_0 of an "interaction-free" reference compound (e.g., for Fe(III): (NH₄)₂NaFeF₆ = spin-only d⁵).

indicating how their and other reference moments μ_0 may be represented analytically. For ions not listed, such as the d^3 and d^5 electronic configurations which have A ground levels, the spin-only moments have been taken as reference in calculating the normalized values μ_{eff}/μ_0 . The d^5 example of $(\text{NH}_4)_2\text{NaFeF}_6$, an elpasolite obeying the Curie law,³² shows that this is justified. Its μ_{eff}/μ_0 plot vs. temperature in Fig. 3 coincides with the line at unity, parallel to the temperature axis, which represents spin-only μ_0 behavior. Departures from this reference line give, irrespective of the changing cation, a good comparative estimate of the degree of magnetic interactions in different compounds. This is illustrated in Fig. 3 by the moment reduction found in the antiferromagnets KFeF_4 and K_2NiF_4 , to be commented on later.

Unless otherwise stated, the magnetic data discussed in the following represent unpublished measurements from our own laboratory. Most experimental details may be found in the theses of Binder,¹⁴ Griebler¹⁵ and Hartung.¹⁶

IV. MAGNETIC BEHAVIOR OF 3d TRANSITION METAL FLUORIDES

A. Influence of Structure on Magnetic Interactions

1. Varying Dimensionality

The most important structural condition for the development of superexchange interactions, at least strong ones, is the presence of ligand bridges between the paramagnetic centers in a compound. The isolated octahedra in elpasolites like $(\text{NH}_4)_2\text{NaFeF}_6$ have already been mentioned as an example of unaltered spin-only magnetism.³²

The first step in a transition from this isolated or zero-dimensional case to three-dimensional bridging is, neglecting dinuclear complexes like $\text{Cs}_3\text{Fe}_3\text{F}_9$,³³ and polynuclear ones, the formation of a chain structure. This is found, e.g., in K_2FeF_5 , where one-dimensional *cis* corner-sharing of octahedra occurs.³⁴ The next step, in which linking via corners goes into two dimensions, is known from the layer structure of KFeF_4 .¹³ The influence of this structural variation on the magnetic properties is obvious from Fig. 4. It is

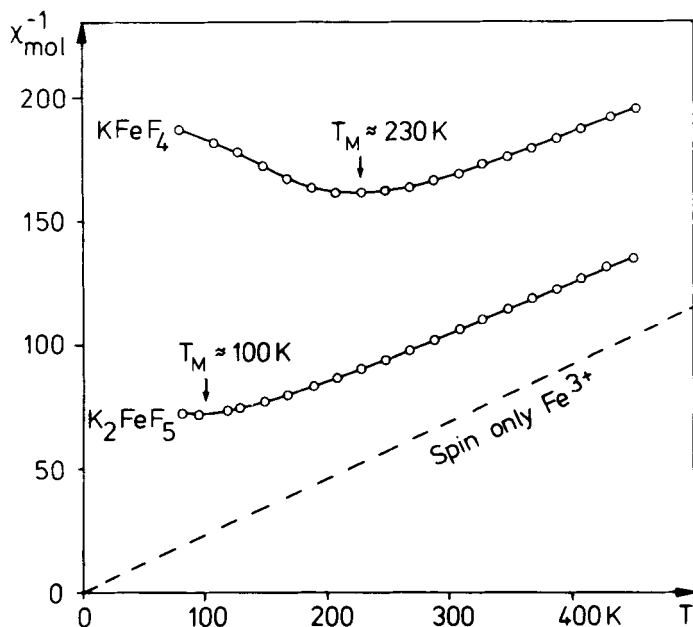


FIGURE 4 Reciprocal susceptibilities (with minima at T_M) of one-dimensional K_2FeF_5 and two-dimensional $KFeF_4$.

interesting to note that the reciprocal susceptibility plots show minima at temperatures T_M of 100 and 230 K, resp., roughly reflecting the 1:2 ratio of the bridging dimensionality in both compounds, in which the average bridge angles Fe-F-Fe are about the same, 170° and 168° , resp.

The $K_2NiF_4/KNiF_3$ couple shown in Fig. 5 is a long-known example illustrating the transition from two- to three-dimensional linking and hence superexchange.¹⁰ Once more the ratio of the temperatures T_M of minimum χ^{-1} , 220 K : 300 K, is in good accordance with the 2:3 relation of bridges, which in this case all are linear.

2. Varying Bridge Angles

Figure 6 shows the magnetic behavior of three copper compounds, as correlated with the Cu-F-Cu bridge angles found in their structures.^{14,35,36} Though $KCuF_3$ and $NaCuF_3$ are perovskites, in which

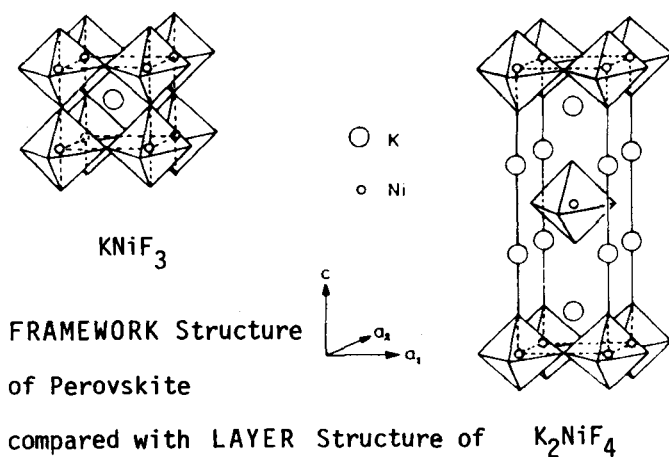
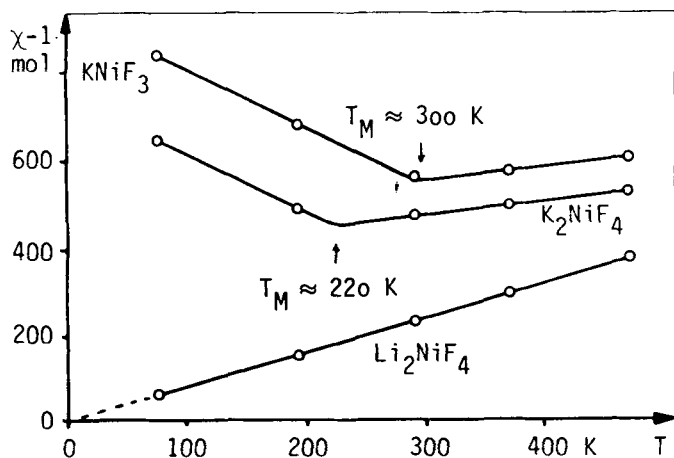


FIGURE 5 Reciprocal susceptibilities (with minima at T_M) and crystal structures of KNiF_3 and K_2NiF_4 . The inverse spinel compound Li_2NiF_4 exhibits normal behavior.

the octahedra are corner-linked in all three dimensions, superexchange becomes possible in them only in one dimension. This is because the electronic configuration $d^9 = t_{2g}^6 d_{z^2}^2 d_{x^2-y^2}^1$ of Cu(II) provides only one half-filled orbital $d_{x^2-y^2}$ and by means of Jahn-Teller distortion and antiferrodistortive ordering⁹ only one-dimen-

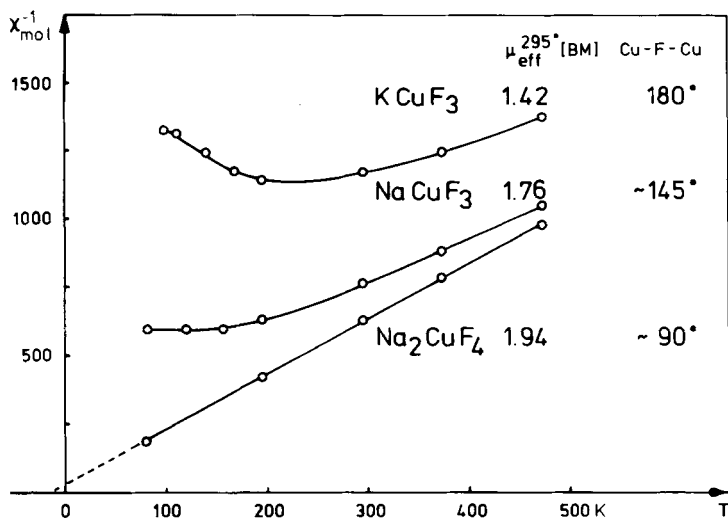


FIGURE 6 Reciprocal susceptibilities of KCuF_3 , NaCuF_3 and Na_2CuF_4 , correlated with the Cu-F-Cu bridge angle.

sional overlap of these with anion p orbitals. In the triclinically distorted NaCuF_3 perovskite the bridging angle of only about 145° in the corresponding direction obviously weakens the magnetic intrachain interactions compared with the linear case of KCuF_3 .

In the different chain structure of Na_2CuF_4 the octahedra share edges rather than corners.³⁶ The bridges are therefore not far from right angles and only normal paramagnetism is observed for this compound. This is also true for Li_2NiF_4 , which as an inverse fluoro-spinel contains all the nickel ions in edge-sharing octahedra.¹⁰ The fact that the magnetic behavior of these fluorides, Na_2CuF_4 and Li_2NiF_4 , does not deviate significantly from that of the corresponding cations in isolated surroundings, e.g., in hexahydrates,^{10,11,37} justifies using them as reference compounds for μ_0 (see Table I).

It may be derived from these observations that there are negligible interactions at 90° and maximum ones at 180° bridges. This tendency is also obvious from Fig. 7, where the exchange energies evaluated for some Mn(III) chain compounds, all consisting of *trans* corner-connected octahedra, are plotted vs. the bridge angles varying within a broad range.³⁸

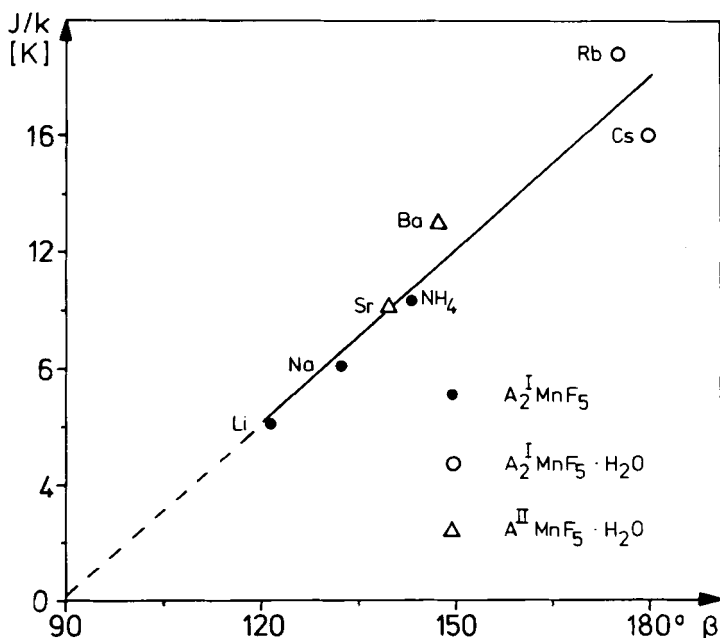


FIGURE 7 Exchange energy and bridge angle $\beta = \text{Mn-F-Mn}$ in some Mn(III) fluoride chain compounds (Ref. 32).

Face-sharing of octahedra makes the bridge angle even smaller than 90° . In this case, too, fluorides generally seem to develop only negligible superexchange interactions of the simple antiferromagnetic type. But ferromagnetic interactions, presumably including direct ones as well, become possible provided the cations approach sufficiently. The ferromagnetic interaction in a chain, as observed at low temperature in the chain structure of CsNiF_3 , may be mentioned as an example of this.^{12,27,39} However, above about boiling nitrogen temperature, there is only poor indication of ferromagnetic effects, even in CsNiF_3 , where the intercationic distances are the shortest ($\text{Ni-Ni} = 262.1 \text{ pm}$) of all related transition metal fluorides.^{9,40,41}

A different situation is found in hexagonal RbNiF_3 , where face-sharing units Ni_2F_9 ($\text{Ni-Ni} = 272.7 \text{ pm}$) are interconnected by single octahedra via linear bridges. The antiferromagnetic coupling effected by the latter is insufficient to compensate for the moment

of the Ni_2F_9 groups, as in these the cations have parallel spins. So the result is ferrimagnetism for RbNiF_3 , corresponding to the unbalanced ratio 1:2 of nickel atoms in two distinct crystallographic positions.^{10,27,41,42} The ferrimagnetism of chiolites like $\text{Na}_5\text{Fe}_3\text{F}_{14}$ ^{27,43} originates from the same principle of different numbers of atoms in antiferromagnetically coupled positions.

CsMnF_3 , however, though isostructural to RbNiF_3 , is antiferromagnetic.⁴⁴ This demonstrates the influence of electronic configuration and/or cation–cation separation ($\text{Mn–Mn} = 299.5 \text{ pm}$)⁴⁰ on the magnetic coupling within face-sharing units, which may be parallel or antiparallel, but in either case is weaker than in corner-linking.

3. Conclusions on Geometric Influences

The correlations sketched above between structure and magnetism strongly support the superexchange model mentioned before. They hint at a predominance of σ -transfer in fluorides, because the maximum interaction found for linear M–F–M arrays then simply follows from the maximum σ overlap given under these conditions for the e_g orbitals of the cation and the p orbitals of the anion. This overlap decreases with increasingly bent bridge and vanishes at right angles. However, another interaction path opens in this second direction, if corner-sharing is also present in the other dimension. Of course an optimum situation is then achieved for three-dimensional linking of octahedra via corners, provided the electronic configuration of the central cation is able to take advantage of it by empty or half-filled orbitals. Contrary to Cu(II) d^9 , this is the case for Ni(II) $d^8 = t_{2g}^6 e_g^2$. The rocksalt arrangement in spin ordering, the so-called G-type found for the magnetic structure of the KNiF_3 perovskite, but not for KCuF_3 ,⁴⁵ demonstrates the importance of electronic configuration and gives some reality to the superexchange model used.

To sum up the influences of dimensionality and bridge angles discussed so far, some nickel compounds are shown in Fig. 8. The sequence of curves in the χ^{-1} vs. T plot does not simply follow the F:Ni stoichiometry of the different compounds because their structures are too different. In addition to corner-sharing, some contain edge- or face-sharing octahedra as well. Since these do not favor the most important σ -superexchange because of 90° bridges

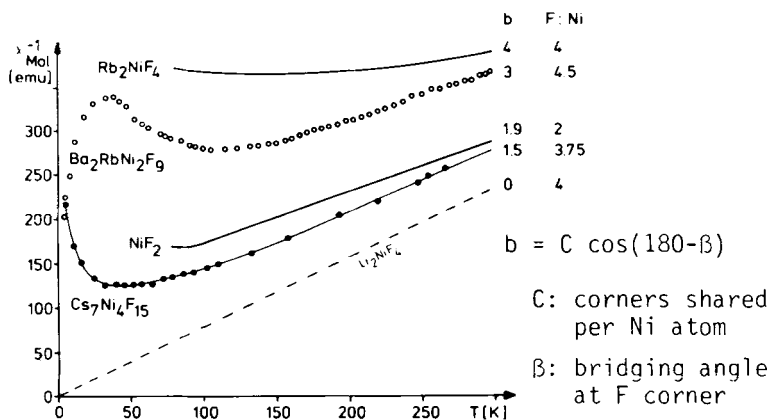


FIGURE 8 The sequence of reciprocal susceptibilities of some Ni(II) fluorocompounds does not follow the F:Ni stoichiometry, but rather the structural "bridge factor" b .

or less, they can be neglected here and only the number C of corners shared per nickel atom remains to be counted and averaged. On the basis of the frequency of σ bridges thus obtained, the dimensional influence is considered for a given compound. The bridge angle influence is regarded by the cosine function of the average angle β at the shared corners. In fact, the simple combination of both magnitudes to a "bridge factor" $b = C \cos(180 - \beta)$ leads to figures which are in good qualitative agreement with the sequence of the susceptibility curves observed.⁴⁰

B. Influence of Cation Properties on Magnetic Interactions

The different 3d transition metal cations active in magnetic interactions may be characterized by their electronic configuration, their charge, and their size. All these are inherent ionic properties, which therefore are not variable *ad libitum*. But by comparing the magnetic properties of isostructural compounds, some trends may be separated according to the properties mentioned. A prerequisite to do this is the choice of high-symmetry framework-structured compounds, in order to avoid any dimensional restriction imposed by the lattice.

We therefore concentrate in the following on isostructural compounds $\text{CsM}^{\text{II}}\text{M}^{\text{III}}\text{F}_6$ having the modified pyrochlore structure of

the cubic RbNiCrF_6 type. The three-dimensional corner-linking of octahedra in this structure is compared to others in Fig. 9. Though in RbNiCrF_6 -type compounds the fluoride bridges are considerably bent ($\text{M-F-M} \approx 140^\circ$) and hence less favorable for superexchange interactions, an exceptional advantage of these pyrochlores is the random distribution of both M(II) and M(III) cations on identical and invariant crystallographic positions.^{9,46,47} Combining para- and diamagnetic M species in $\text{CsM}^{\text{II}}\text{M}^{\text{III}}\text{F}_6$ compounds, it becomes possible to compare the behavior of M(II) and M(III) transition metal ions under constant conditions of structure and magnetic dilution. It will be demonstrated first, how diamagnetic dilution, inevitable in this case, influences superexchange in pyrochlores and related structures.

1. Varying Magnetic Dilution

In Fig. 10 the μ_{eff}/μ_0 curves of three compounds differing in cobalt(III) content are drawn. The uppermost curve of the most diluted pyrochlore, CsMgCoF_6 , shows that appreciable moment reduction, indicative of antiferromagnetic interactions, is already

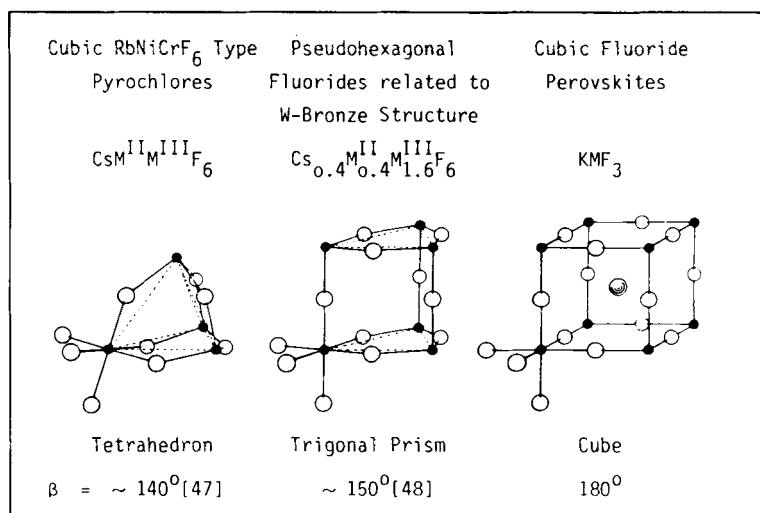


FIGURE 9 The smallest units of corner-sharing octahedra and average bridge angles β in the framework structures of pyrochlore, hexagonal tungsten bronze and perovskite.

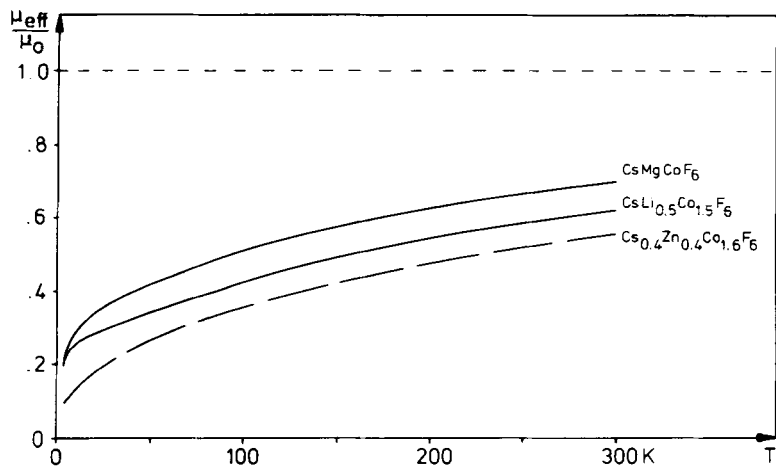


FIGURE 10 The effect of magnetic dilution in Co(III)pyrochlores CsMgCoF_6 and $\text{CsLi}_{0.5}\text{Co}_{1.5}\text{F}_6$ compared to the tungsten bronze structured compound $\text{Cs}_{0.4}\text{Zn}_{0.4}\text{Co}_{1.6}\text{F}_6$ (Refs. 16 and 17).

significant at the 50% dilution level, which is the standard for the examples in the later sections. The higher cobalt content in the isostructural pyrochlore $\text{Cs}(\text{Li}_{0.5}\text{Co}_{1.5})\text{F}_6$ only causes a shift towards still lower μ_{eff}/μ_0 values: A similar shift is also observed for the compound $\text{Cs}_{0.4}(\text{Zn}_{0.4}\text{Co}_{1.6})\text{F}_6$, in which the cobalt concentration is but slightly higher. The change is in fact mostly attributable to the different structure of this phase. It is of the tungsten bronze related $\text{Cs}_{0.4}(\text{Zn}_{0.4}\text{Fe}_{1.6})\text{F}_6$ type,^{16,17,48} in the network of which, built up from three-dimensionally corner-sharing octahedra as well, less bent bridges (average $\sim 150^\circ$) offer better superexchange conditions than in the pyrochlores (see Fig. 9).

The influence of varying diamagnetic substitution in the bronze phase of the iron compound mentioned is obvious in Fig. 11.

2. Varying Ionic Charge

Isoelectronic representatives, like the d^5 compounds CsMnGaF_6 and CsZnFeF_6 , are appropriate for studying the effect of varying ionic charge on the intensity of magnetic interactions. This is shown in Fig. 12, where another example, d^8 of CsNiGaF_6 and CsZnCuF_6 , is added. It can be seen in both cases that the higher-charged cations, Fe(III) and Cu(III), respectively, effect stronger moment

reductions than the lower-charged ones, Mn(II) and Ni(II), respectively. However, the inherent size difference between the iso-electronic, but differently charged ions may contribute to this appearance, though the inverse size relation of the diamagnetic counterpart ions should greatly compensate for this change, so as to make the lattice constants of the compounds not too different. Nevertheless the size influence should be studied separately and for cations of the same valence state.

3. Varying Ionic Size

The sequence of μ_{eff}/μ_0 curves in Fig. 13 for some bivalent transition metal ions is $\text{CsMnGaF}_6 > \text{CsNiGaF}_6 > \text{CsCuGaF}_6$, which is not the generally accepted order of ionic sizes. There is no doubt regarding the volume sequence $\text{Mn} > \text{Cu} > \text{Ni}$, and that of the radii is the same.^{49,50} However, it should be borne in mind that the Jahn–Teller ion Cu(II) displays, so to speak, two different radii. Only the smaller one, corresponding to the shorter Cu–F axes found in Jahn–Teller distorted compounds, is relevant in the present context. The reason for this is that the shorter axes cor-

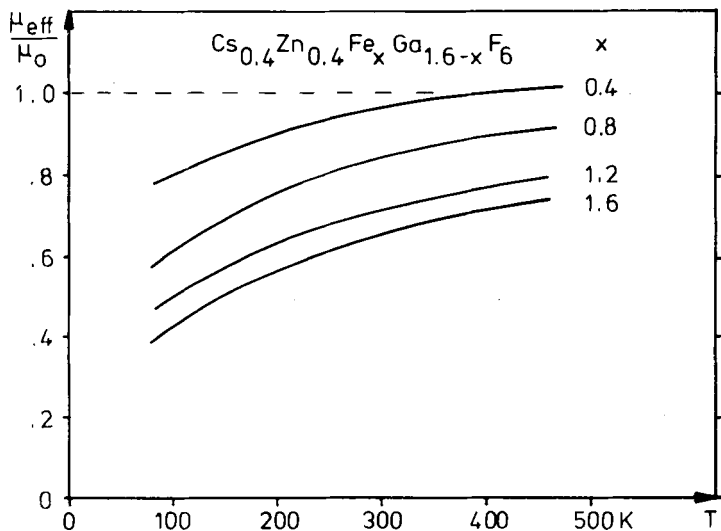


FIGURE 11 The effect of magnetic dilution in the tungsten bronze related structure of $\text{Cs}_{0.4}\text{Zn}_{0.4}\text{Fe}_{1.6}\text{F}_6$ (Refs. 14 and 48).

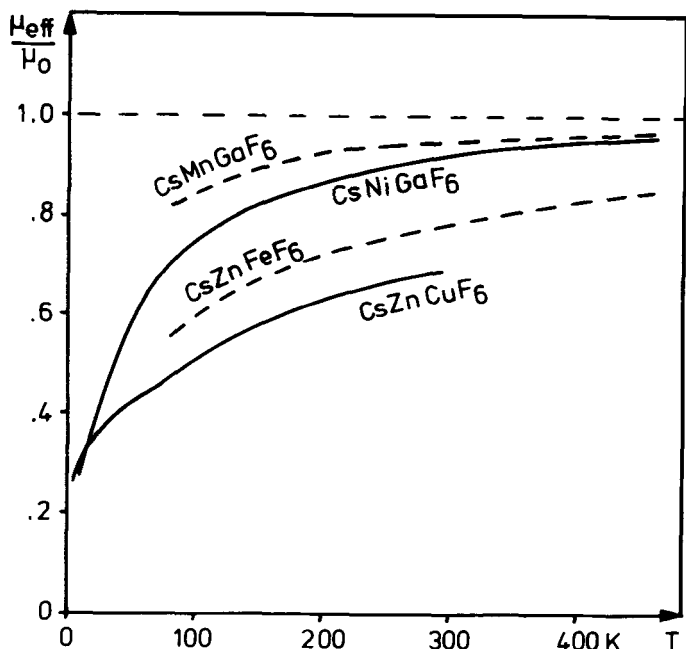


FIGURE 12 Charge influence on magnetic interactions in the isoelectronic systems d^5 : CsMnGaF_6 ($a = 1040.6$ pm)/ CsZnFeF_6 ($a = 1039.6$ pm) and d^8 : CsNiGaF_6 ($a = 1025.8$ pm)/ CsZnCuF_6 ($a = 1025.2$ pm).

respond to the orientation of the half-filled $d_{x^2-y^2}$ orbital, which is the only one in the d^9 system capable of superexchange. Though in cubic copper(II) pyrochlores a dynamic Jahn–Teller effect seems to be operating, the short distances known from statically distorted compounds should apply as far as magnetic interactions are concerned. The sequence then becomes ($\text{Mn-F} \approx 212$ pm) $>$ ($\text{Ni-F} \approx 200$ pm) $>$ ($\text{Cu-F} \approx 192$ pm),^{51,40,52} quite in accordance with the μ_{eff}/μ_0 gradation observed in Fig. 13.

It should be noted, however, that the curves of nickel and copper compounds are nearly identical in the case of the fully paramagnetic pyrochlores CsNiFeF_6 and CsCuFeF_6 . This is not contrary to the above arguments, if the inherent dimensional restrictions of the d^9 configuration, already mentioned before, are considered. These restrictions are only obscured at the magnetically diluted compounds, in which the number of paramagnetic neighbors is less than a dynamic Jahn–Teller ion might involve in interactions.

The simple correlation: shorter (or more) bonds, stronger interactions, seems not to be followed by the example of CsZnCoF_6 and CsZnCuF_6 , also illustrated in Fig. 13. The lower μ_{eff}/μ_0 curve of the larger cation Co(III) ($r \approx 61$ pm; $d^6 = t_{2g}^4 e_g^2$) hints at the possibility that additional superexchange pathways, perhaps via bonds of π character, which cannot form in the case of Cu(III) ($r \approx 57$ pm; $d^8 = t_{2g}^6 e_g^2$), may contribute to the observed overall reduction of moments. Therefore, last but not least, the influence of the number of unpaired electrons, i.e., of electronic configuration, should be considered.

4. Varying Electronic Configuration

a. Symmetric Superexchange. The main distinction among octahedrally coordinated high-spin 3d transition metal ions may be made, in view of the assumption of predominant σ superexchange, according to the most relevant e_g orbital occupation. The highest symmetric species are the $d^3 = t_{2g}^3 e_g^0$ and $d^5 = t_{2g}^3 e_g^2$ configurations,

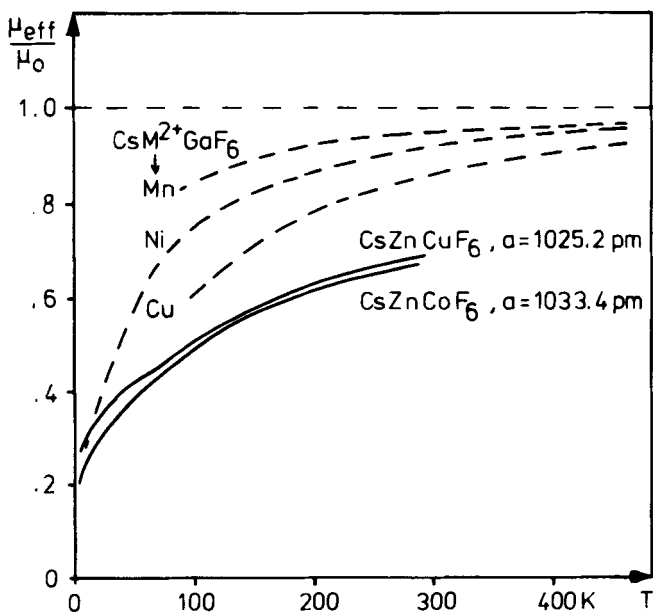


FIGURE 13 Size influence on magnetic interactions in some pyrochlores $\text{CsM}^{\text{II}}\text{GaF}_6$ and $\text{CsZnM}^{\text{III}}\text{F}_6$. ($\text{M}^{\text{II}} = \text{Mn, Ni, Cu}$; $a = 1040.6, 1025.8, 1028.9$ pm. $\text{M}^{\text{III}} = \text{Co, Cu}$; $a = 1033.4, 1025.2$ pm) (Ref. 50).

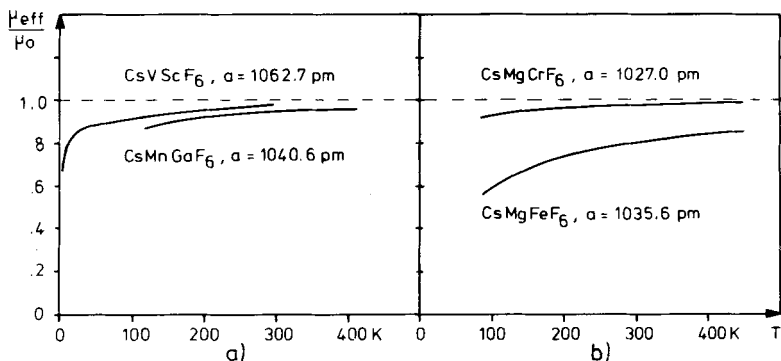


FIGURE 14 The influence of electronic configuration on magnetic interactions in d^3/d^5 systems of (a) divalent and (b) trivalent transition metal ions.

which are compared in Fig. 14 for both bi- and trivalent ions V(II)/Mn(II) and Cr(III)/Fe(III), respectively, where the pair constituents have about similar sizes. In both valence states the isoelectronic e_g^2 species show a stronger moment reduction than the e_g^0 species. But the difference is much greater for the trivalent ions.

A questionable π contribution to superexchange remains undetected as long as the t_{2g} configuration remains the same. In the Co(III)/Cu(III) example of the foregoing section, however, the unlike t_{2g} configuration of the cations makes a differentiation possible, and justifies the postulation of the presence of additional, but weaker, π interactions if empty or half-filled t_{2g} orbitals are available.

Judging from the gradation observed, it may be said that electronic configurations containing half-filled orbitals in either set, e_g or t_{2g} , but much less in the latter case, considerably enhance superexchange interactions compared to those which take place if the corresponding orbitals lack their "own" electrons.

b. Asymmetric Superexchange. A special, hitherto neglected, case is the asymmetric superexchange of half-filled orbitals interacting, via the anion, with empty ones. It has already been pointed out that ferromagnetic spin coupling results under these conditions (cf. Fig. 1). Well-known examples are the A type magnetic structures found in the d^4 compounds MnF_3 and KCrF_3 , where Jahn–Teller-induced orbital ordering is such that half-filled $d_{z^2}^1$ interact with

empty $d_{x^2-y^2}^0$ orbitals to generate ferromagnetic layers, which finally couple antiparallel via the remaining perpendicular lobes of the $d_{x^2-y^2}^0$ orbitals.^{2,8,45,53,54}

In fact, it was the intention to combine cations with e_g^2 and e_g^0 electronic configurations to form ferromagnetic “perovskites” that resulted in the detection of pyrochlores like RbNiCrF_6 .^{46,47} Unfortunately the pyrochlores lack the cation order required to interact ferromagnetically on a long-range scale. However, depending on preparative conditions, samples have been sporadically obtained in which enhanced magnetic moments indicative of ferromagnetic contributions were observed (see Fig. 15).¹⁴ The underlying problem of partial and varying cation ordering is avoided in

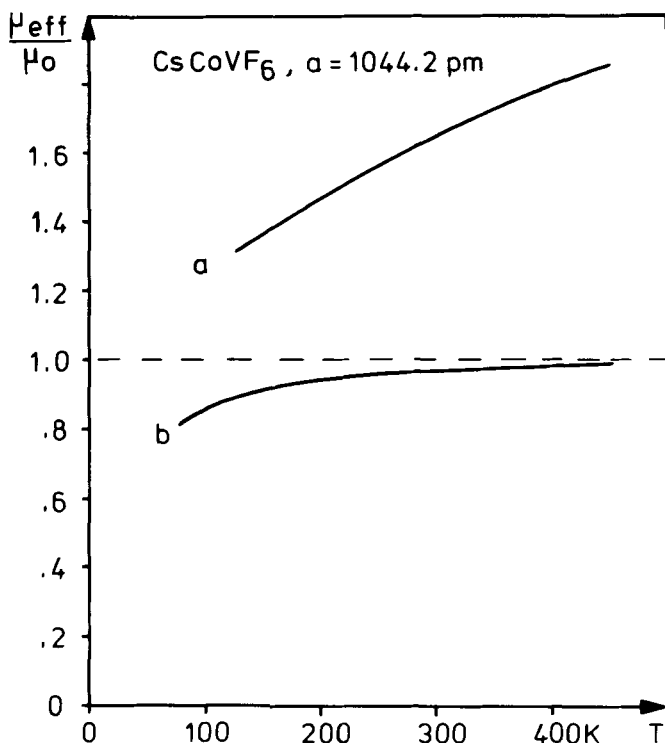


FIGURE 15 Influence of preparative conditions on the magnetism of CsCoVF_6 : (a) Sample prepared at 600°C and slowly cooled; (b) the same sample reheated at 800°C and quenched.

the magnetically diluted compounds discussed here which contain only one paramagnetic species. The absence of magnetic long-range ordering in pyrochlores is caused by frustration^{55,56} of spins interacting within regular arrays of triangles and tetrahedra. This property makes compounds like CsNiFeF_6 interesting as spin glasses,^{57–59} where it is possible to use the observed moment variations as a relative measure of the intensity of short-range interactions.

Figure 16 shows that in the case of d^1 and d^2 configurations, as present in CsZnTiF_6 and CsMgVF_6 , resp., enhanced moments are observed. This is another indication of π superexchange being active, at least in the lower temperature range: Provided that the t_{2g} level splitting is negligible, the configurations mentioned imply the possibility not only of interacting antiferromagnetically, e.g., $d_{xy}^1-d_{xy}^1$, but also in an unsymmetric way, $d_{xy}^1-d_{xy}^0$, which would result in ferromagnetic contributions (cf. Fig. 1) and explain the behavior found. The same mechanism is claimed for the ferromagnetism of CrO_2 .⁶⁹

The bent bridges in the pyrochlores seem disadvantageous only as far as σ superexchange is concerned, which is strong only for e_g^2 systems. At the same time, t_{2g} orbitals find ameliorated conditions for overlap with anion orbitals in this structure (see Fig. 1). Even though σ transfer still dominates the exchange coupling mechanism, π superexchange is more important here than in linear fluoride-bridged systems.

5. Conclusions on Ionic and Electronic Influences

The sequence of the μ_{eff}/μ_0 curves of the “half-magnetic” pyrochlores, compiled in Fig. 17, may be used to arrange the paramagnetic ions in a series of increasing magnetic coupling strength. This is done in Table II which also includes some ionic and electronic data that were used above in explaining the different influences. These influences result in the subdivision into three groups of ions, as is obvious from Fig. 17: The trivalent cations divide into the groups of weakest and strongest coupling, corresponding to empty and half-filled e_g orbitals, respectively, in their d electron shell. The third group of intermediate coupling strength, falling between the two others, is that of the bivalent cations, all with e_g^2 (or even e_g^3) configurations.

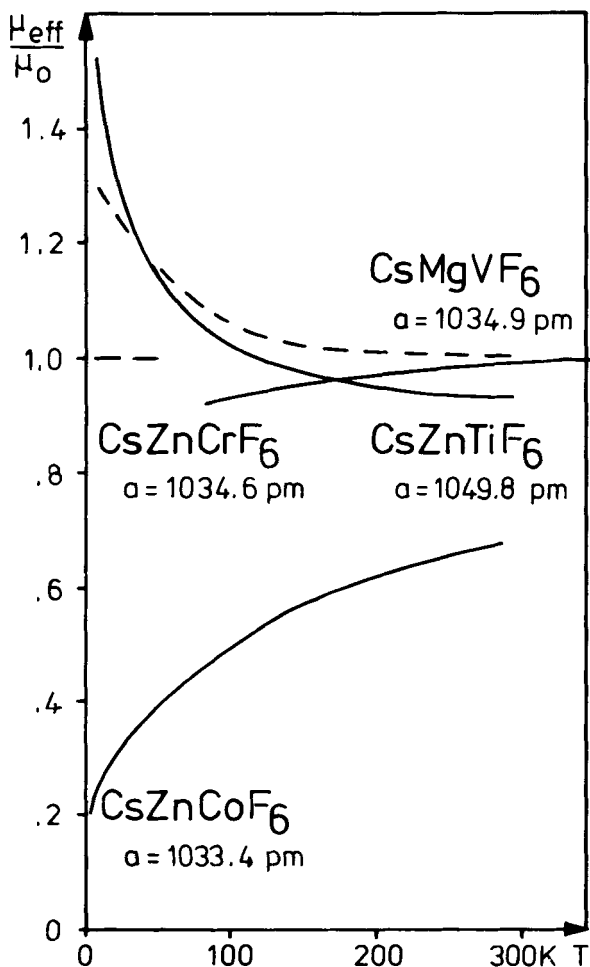


FIGURE 16 Enhanced magnetism in d^1 and d^2 pyrochlores compared with the reduction observed in d^3 and d^6 systems.

In good accordance with chemical bonding ideas, the gradation observed indicates the electronic configuration, especially of the e_g orbitals, as the most important factor in superexchange, followed by the influence of charge, an increase of which also increases covalency. The smaller influences of t_{2g} orbital occupation, i.e., π

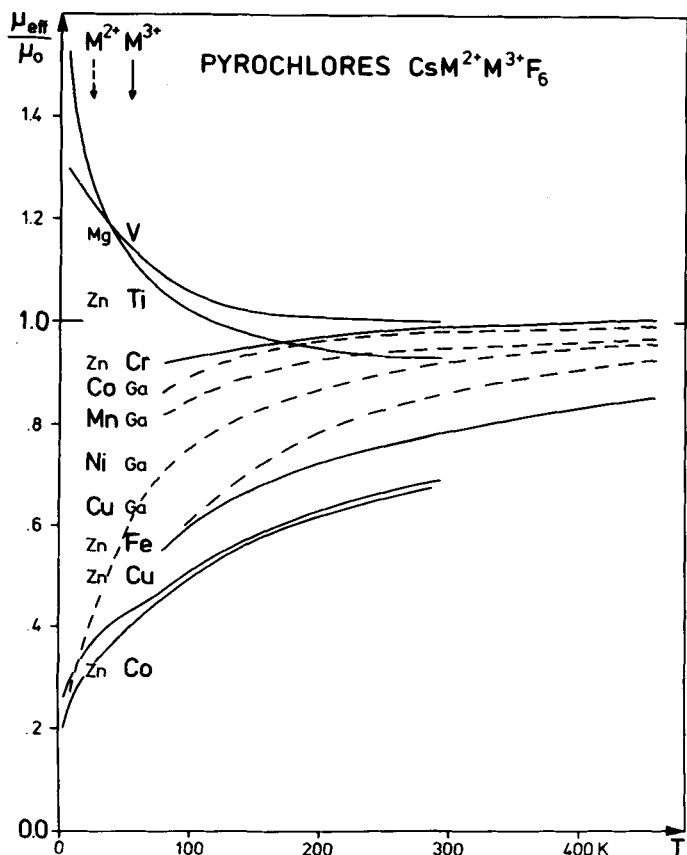


FIGURE 17 Sequence of μ_{eff}/μ_0 curves for M(II), resp., M(III) ions of 3d transition metals in pyrochlores $\text{CsM}^{\text{II}}\text{M}^{\text{III}}\text{F}_6$.

contributions, and of ionic size, i.e., bond length, are such as to modify the behavior dominated by the first-mentioned factors.

The validity of the series is limited, however, to fluorides and to the structural conditions given in pyrochlores. But the curves in Fig. 18 show that in the related bronze-like structure, quoted above, about the same gradation is found for the trivalent transition metal cations. (The bivalent ones are too dilute in this structure to give very significant results.) That no ferromagnetic contributions are detected here in the case of Ti(III) and V(III) may be

TABLE II

Series of increasing antiferromagnetic coupling strength for 3d transition metal ions in cubic pyrochlores $\text{CsM}^{2+}\text{M}^{3+}\text{F}_6$ (the other M cation being diamagnetic). The ionic and electronic data given suggest, in the order of increasing importance, the following influences on the coupling strength: $t_{2g}^0 < t_{2g}^6$, $r_{\text{large}} < r_{\text{small}}$, $\text{M}^{2+} < \text{M}^{3+}$, $e_g^0 < e_g^2$

Ion	Ti^{3+}	V^{3+}	V^{2+}	Cr^{3+}	Co^{2+}	Mn^{2+}	Ni^{2+}	Cu^{2+}	Fe^{3+}	Cu^{3+}	Co^{3+}
Electronic Configuration	d^1	d^2	d^3	d^3	d^7	d^5	d^8	d^9	d^5	d^8	d^6
e_g	0	0	0	0	2	2	2	3	2	2	2
t_{2g}	1	2	3	3	5	3	6	6	3	6	4
r (pm) [49]	67	64	79	61.5	74.5	83	69	73	64.5	—	61
r (pm) [50]	68.6	64.8	75	61.4	72.6	78	69	70.7	64.5	56.6	60.9
M-F (pm) [9]	197	193	205	190	203	212	200	192*	193	188	190

*Referred to the four shorter bonds (corresponding to half-filled $d_{x^2-y^2}$ orbital orientation) in Jahn–Teller distorted octahedra.

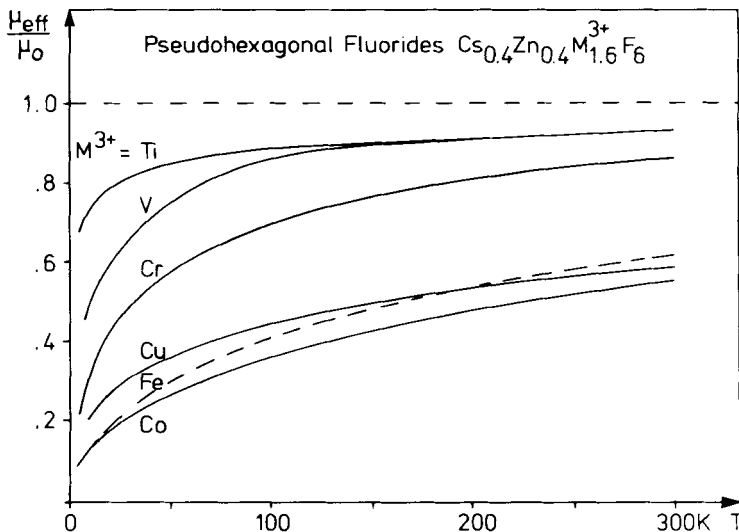


FIGURE 18 Sequence of μ_{eff}/μ_0 curves for M(III) transition metal ions in fluoride "bronzes" $\text{Cs}_{0.4}\text{Zn}_{0.4}\text{M}_{1.6}^{3+}\text{F}_6$.

explained by appreciable splitting of the t_{2g} level in the pseudo-hexagonal structure, also indicated by spectroscopic measurements.^{16,17}

Finally, it should be mentioned that the pyrochlores offer another possibility for magnetic comparison: that of the influence of the anions, if fluorine is stepwise substituted by oxygen. All intermediate oxide/fluoride compositions $\text{CsMM}'\text{O}_{6-x}\text{F}_x$ between oxides like CsNbWO_6 and fluorides like CsZnFeF_6 are known and studies of appropriate magnetic substitution is suggested.^{9,46,60}

V. MAGNETIC BEHAVIOR OF SELECTED 3d TRANSITION METAL CYANIDES

One of the most important differences between the halide ions and cyanide as a pseudo-halide ligand is the strong field effect of the latter, which results in low-spin states. With some exceptions,⁶¹⁻⁶³ the magnetic behavior of cyanides has attracted little attention, which is understandable as far as diamagnetic species

are concerned, since they need no further confirmation. On the other hand, there may still be unpaired electrons in low-spin states and the question of possible interactions of these seems interesting, if at the same time the ambident nature of the cyanide ligand is considered, frequently leading to linearly bridged systems. Therefore, we have also studied the structural and magnetic properties of a series of cyanides. The compositions selected were always $A^I M^{II} M^{III} (CN)_6$, formally like the pyrochlores $CsM^{II} M^{III} F_6$, but additionally hydrated in some cases and with different structures in all.

A. Structures of Some Cyanides $A^I M^{II} M^{III} (CN)_6 \cdot nH_2O$

1. Framework Structure of Cyanides $CsM^{II} M^{III} (CN)_6$

Contrary to the fluorides of analogous composition, the cyanides adopt the perovskite structure. Even though cation deficient, this structure is stabilized by linear cyano bridges in its three-dimensional framework. Potassium compounds like the "soluble prussian blue," $KFe_2(CN)_6$, with Fe(II) C-coordinated have been known for a long time.⁶⁴ In some cubic cesium compounds $CsM^{II} M^{III} (CN)_6$ the higher-valent species $M(III) = Cr, Fe, Co$ bind at the carbon end while divalent ions like $M(II) = Mn, Ni, Zn$ bind at the N side of the cyano bridges as determined by spectroscopic and magnetic studies.^{15,19} $CsMnCr(CN)_6$ proved to be ferrimagnetic, as discussed later.

2. Layer Structure of $NMe_4MnCr(CN)_6 \cdot 4H_2O$

Cations essentially larger than cesium no longer fit in cubic perovskite cages, and as a result these are blown up in one dimension and persist only in the remaining two, as shown in Fig. 19 for $NMe_4MnCr(CN)_6 \cdot 4H_2O$. The large tetramethylammonium cations and water of crystallization are incorporated between the layers. Half of the waters are directly transcoordinated to manganese and substitute for the N ends of two cyano ligands. These are missing here because the layer separation has removed two axial of the six surrounding $Cr(CN_6)^{3-}$ anions: The $CsMnCr(CN)_6$ framework with six anions providing all six coordination positions to form MnN_6 has changed to layers containing $MnN_4(H_2O)_2$. The remaining equatorial cyano bridges are no longer strictly linear (average Mn-NC-Cr: 171° at N).^{21,65}

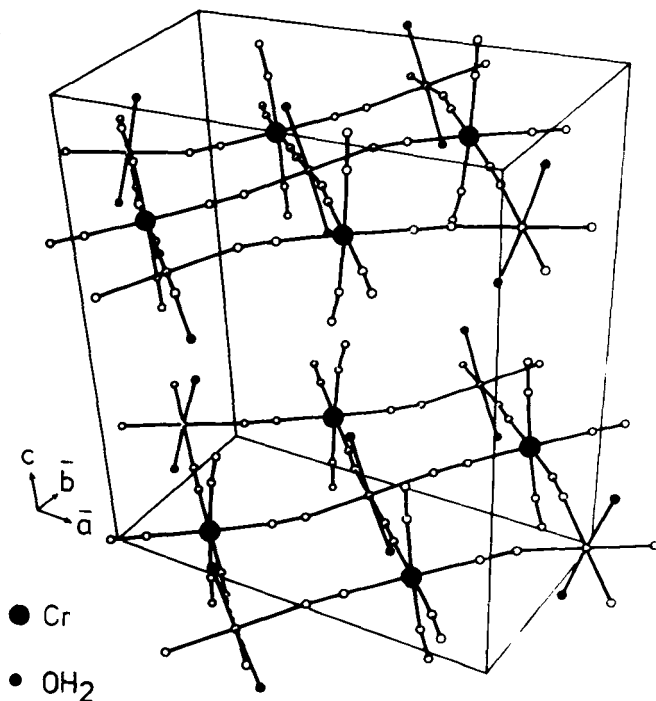


FIGURE 19 Layer structure of $\text{NMe}_4\text{MnCr}(\text{CN})_6 \cdot 4\text{H}_2\text{O}$ (Ref. 65). The interlayer ions NMe_4^+ and crystal water molecules not coordinated to $\text{Mn}(\text{II})$ have been omitted for clarity.

3. Chain Structure of $\text{NMe}_4\text{MnM}^{\text{III}}(\text{CN})_6 \cdot 8\text{H}_2\text{O}$ ($\text{M}^{\text{III}} = \text{Mn}, \text{Fe}, \text{Co}$).

Changing from the larger $\text{Cr}(\text{III})$ ion to the smaller low-spin cations $\text{Mn}(\text{III})$, $\text{Fe}(\text{III})$ or $\text{Co}(\text{III})$, the process of perovskite destruction by tetramethylammonium ions is two-dimensional, and only one-dimensional bridging, linear in this case, persists. Octahedral hexacyano anions $\text{M}(\text{CN})_6^{3-}$ and square tetra-aquo cations $\text{Mn}(\text{H}_2\text{O})_4^{2+}$ are stacked to form the chain structure shown in Fig. 20.⁶⁶ The resulting manganese coordination $\text{MnN}_2(\text{H}_2\text{O})_4$ is just the inverse of that found in the layer structure sketched before.

B. Magnetism of the Cyanides $\text{A}^{\text{I}}\text{Mn}^{\text{II}}\text{M}^{\text{III}}(\text{CN})_6 \cdot n\text{H}_2\text{O}$

1. Results of Susceptibility and Magnetization Measurements

a. $\text{CsMnCr}(\text{CN})_6$ and $\text{NMe}_4\text{MnCr}(\text{CN})_6 \cdot 4\text{H}_2\text{O}$. The reciprocal susceptibility plots of framework-structured $\text{CsMnCr}(\text{CN})_6$ and of

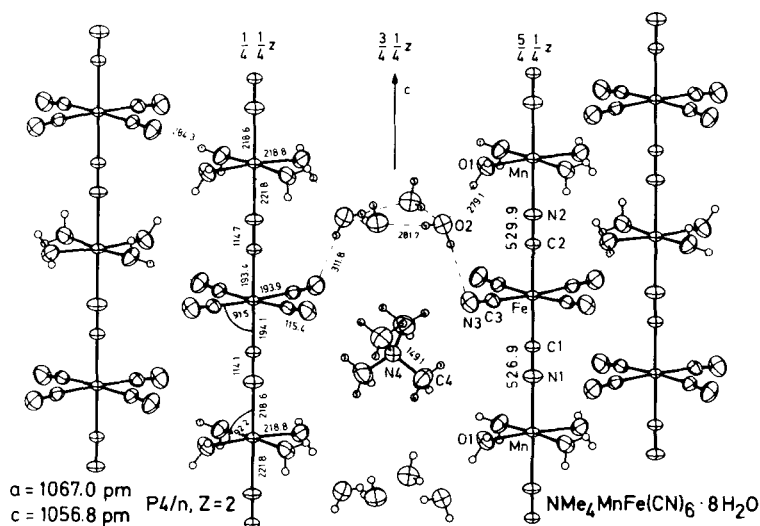


FIGURE 20 Chain structure of $\text{NMe}_4\text{MnFe}(\text{CN})_6 \cdot 8\text{H}_2\text{O}$, also found for $\text{M}^{\text{III}} = \text{Mn, Co}$ (Ref. 66).

the corresponding layer compound $\text{NMe}_4\text{MnCr}(\text{CN})_6 \cdot 4\text{H}_2\text{O}$ follow hyperbolic curves, as shown in Fig. 21.^{19,21} This behavior is typical for ferrimagnetism, the ordering point of which may be calculated from the hyperbola equation adapted to reproduce the observed susceptibilities. This yields the Néel temperatures T_N given in the figure, which happen to display a 3:2 ratio like the bridging dimensionalities do. The spontaneous magnetizations found below the Néel temperatures extrapolate to values near $n_B = 2$ unpaired electrons at absolute zero. These values suggest antiparallel orientations of the unlike spins, corresponding to the high-spin configurations d^5 and d^3 in the bimetallic compounds as the origin of their ferrimagnetism. Another cause of ferrimagnetism, i.e., of uncompensated antiparallel coupling, was mentioned earlier in the discussion of RbNiF_3 , where, rather than the spins being distinct, unlike numbers of nickel atoms occupy two different positions.

b. $\text{NMe}_4\text{MnM}^{\text{III}}(\text{CN})_6 \cdot 8\text{H}_2\text{O}$ ($\text{M}^{\text{III}} = \text{Mn, Fe}$). These two isostructural chain compounds behave differently, as may be seen from their reciprocal susceptibility plots in Fig. 22. Only the mixed-valent manganese cyanide shows the hyperbolic curve, lying higher than the straight line of spin-only behavior, as already known from

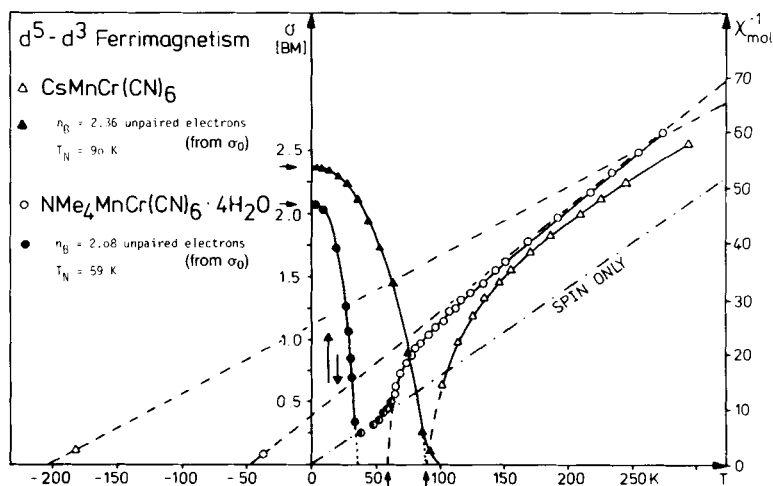


FIGURE 21 Ferrimagnetic behavior and spontaneous magnetization σ_0 of CsMnCr(CN)_6 and $\text{NMe}_4\text{MnCr(CN)}_6 \cdot 4\text{H}_2\text{O}$. The curves drawn in the paramagnetic region through the points measured are the adapted hyperbolae, the asymptotes of which are drawn as dashed lines (Refs. 2, 19 and 21). All values refer to 1 mole of the chemical formula given, i.e., $1 \text{ Mn}^{II} + 1 \text{ Cr}^{III} = 2 \text{ M}$.

the ferrimagnetic framework and layer compounds. The iron chain compound, however, follows the spin-only line, calculated as in the preceding case under the assumption of high-spin Mn(II) , $d^5 = t_{2g}^3 e_g^2$, but low-spin M(III) , $d^4 = t_{2g}^4 e_g^0$ and $d^5 = t_{2g}^5 e_g^0$, respectively.

The magnetization measurements performed on single crystals of both compounds are shown in Fig. 23. $\text{NMe}_4\text{Mn}_2(\text{CN})_6 \cdot 8\text{H}_2\text{O}$ becomes ferrimagnetic at $T_N = 28.5$ K and yields a saturation moment M_s , which corresponds to the difference of high-spin d^5 /low-spin d^4 , $n_B = 3.1 = M_s M_m / N_0 \mu_B$ (M_m : molar mass, N_0 : Avogadro's number, μ_B : Bohr Magneton, $N_0 \mu_B = 5584$ atoms-erg/mole-Gauss).⁷⁰ The iron compound, antiferromagnetic below $T_N = 9.3$ K, undergoes a metamagnetic transition at some critical field of 1.2 Tesla to become ferrimagnetic. Once more the saturation moment in the ferrimagnetic state, corresponding to $n_B = 3.9$ unpaired electrons, suggests antiparallel spin orientation of the two cations, high/low-spin d^5 in this case.²⁰

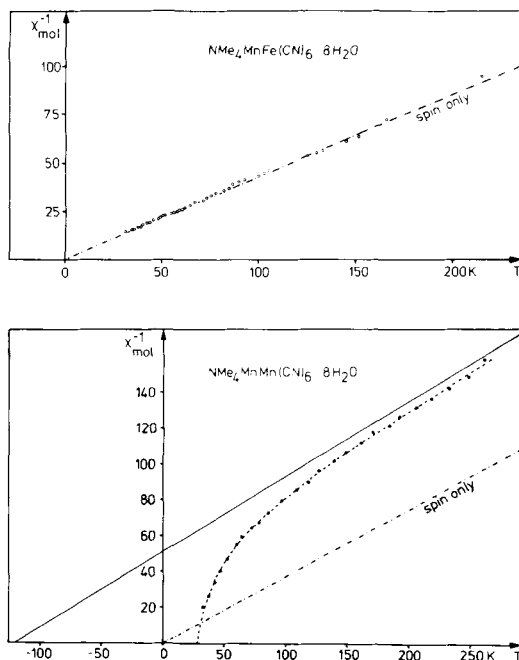
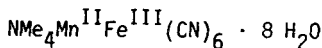
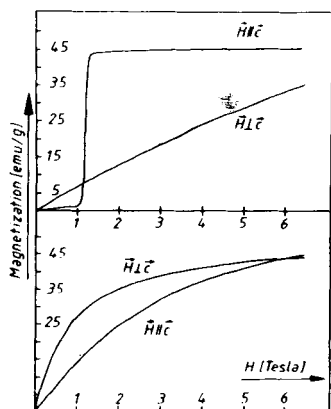


FIGURE 22 Reciprocal susceptibilities of the isostructural chain compounds $\text{NMe}_4\text{Mn}^{\text{II}}\text{Fe}^{\text{III}}(\text{CN})_6 \cdot 8\text{H}_2\text{O}$ and $\text{NMe}_4\text{Mn}^{\text{II}}\text{Mn}^{\text{III}}(\text{CN})_6 \cdot 8\text{H}_2\text{O}$ (Ref. 20). The χ^{-1} values refer to 1 mole content of paramagnetic ions, i.e., $(1/2)(\text{Mn}^{\text{II}} + \text{Fe}^{\text{III}}) = 1$ M and $(1/2)(\text{Mn}^{\text{II}} + \text{Mn}^{\text{III}}) = 1$ Mn, respectively. The curve drawn in the case of the Mn(III) compound is the adapted hyperbola, the full straight line its asymptote.

2. Interpretation of Results

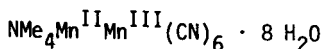
A superexchange mechanism is required to explain the ferrimagnetism observed in the four cyanide compounds. The mechanism should provide antiparallel spin coupling, which, however, cannot use simple σ transfer as in the case of fluorides: The interaction via anion orbitals between half-filled e_g orbitals of high-spin Mn(II) and empty e_g orbitals of the M(III) cations Cr(III), low-spin Mn(III) or Fe(III), resp., according to the Goodenough–Kanamori rules would produce parallel coupling. The “symmetric” overlap required to yield antiparallel spin orientations seems possible only by utilization of t_{2g} orbitals, some of which are half-filled in all four cases. To cause them to interact, π overlap is needed with



$$T_N = 9.3 \text{ K}$$

$$n_B = 3.95 \text{ unpaired electrons at saturation } M_s$$

$$H_{\text{crit}} = 1.2 \text{ Tesla (at 4.2 K)}$$



$$T_N = 28.5 \text{ K}$$

$$n_B = 3.1 \text{ unpaired electrons at saturation } M_s$$

FIGURE 23 Single crystal magnetization curves and saturation moments of $\text{NMe}_4\text{MnM}^{\text{III}}(\text{CN})_6 \cdot 8\text{H}_2\text{O}$, measured at 4.2 K (Ref. 20).

appropriate anion orbitals. In other words, the well-known back-bonding of the cations into empty antibonding π^* orbitals of the cyanide bridge may be assumed to support the superexchange in these cyanide compounds.

This assumption of π superexchange in cyanides is visualized in Fig. 24, along with the ferrimagnetic data for the four compounds under discussion. Data for a fifth compound $\text{Mn}^{\text{II}}\text{Mn}^{\text{IV}}(\text{CN})_6 \cdot x\text{H}_2\text{O}$, is added from the literature.⁶³

The parallelism between ordering temperatures and bridge dimensionalities 1:2:3 in the three compounds $\text{NMe}_4\text{Mn}_2(\text{CN})_6 \cdot 8\text{H}_2\text{O}$, $\text{NMe}_4\text{MnCr}(\text{CN})_6 \cdot 4\text{H}_2\text{O}$ and $\text{CsMnCr}(\text{CN})_6$ is striking, though perhaps accidental. But it suggests the argument that the lower Néel point of the iron chain compound is connected with the fact that low-spin Fe(III) contains but one half-filled t_{2g} orbital, compared to two for the isostructural Mn(III) compound. The latter therefore offers better superexchange conditions, in accordance with its higher Néel point.

More than two t_{2g} orbitals never point in the same direction; therefore to take advantage of all three being half-filled, as is the case in the d^3 Cr(III) compounds, at least a layer or better, a framework structure is required. Such a framework is present not only in $\text{CsMnCr}(\text{CN})_6$ but also in $\text{Mn}^{\text{II}}\text{Mn}^{\text{IV}}(\text{CN})_6 \cdot x\text{H}_2\text{O}$. The lower

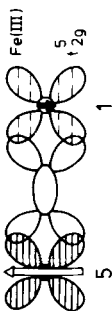
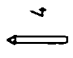
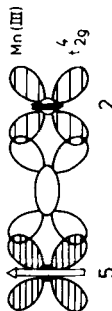
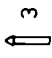

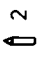
CN-Bridges in Dim.	$Mn^{II}-N\equiv C-M^{III}$		n_B Unpaired Electrons calc.	T_N (K)
	High Spin	Low Spin	obs.	
$NMe_4MnFe(CN)_6 \cdot 8H_2O$	1			3.9 9.3
$NMe_4MnMn(CN)_6 \cdot 8H_2O$	1			3.1 29
$NMe_4MnCr(CN)_6 \cdot 4H_2O$	2			2.1 59
$CsMnCr(CN)_6$	3			2.4 90
$Mn^{II}Mn^{IV}(CN)_6 \cdot xH_2O$ (Eysel et al., 1980)	3			1.9 49

FIGURE 24 Proposal to explain the ferrimagnetism and its gradation observed in cyanides by superexchange via antibonding π^* orbitals of the ligand bridge.

Néel point of the d^3 Mn(IV) compound may then be caused by the poorer back-donation of the isoelectronic, but higher-charged cation.

Further studies are needed, of course, to support or discard this simple and purely qualitative view of structure, bonding, and magnetic interactions.

Acknowledgments

I would like to thank F. Binder, W. D. Griebler, A. Hartung, W. Kurtz, J. Pebler and M. Witzel, who have performed the preparation and measurements of most of the samples reported here. The financial support of the Deutsche Forschungsgemeinschaft and the Fonds der Chemischen Industrie is gratefully acknowledged.

D. BABEL

*Fachbereich Chemie und Sonderforschungsbereich 127
("Kristallstruktur und Chemische Bindung")
der Philipps-Universität,
Hans-Meerwein-Strasse,
D-3550 Marburg,
Federal Republic of Germany*

References

1. W. Klemm, *Magnetochemie* (Akadem. Verlagsgesellschaft, Leipzig, 1936).
2. J. B. Goodenough, *Magnetism and the Chemical Bond*, (Wiley, New York, 1963).
3. A. Weiss and H. Witte, *Magnetochemie* (Verlag Chemie, Weinheim, 1973).
4. F. E. Mabbs and D. J. Machin, *Magnetism and Transition Metal Complexes* (Chapman and Hall, London, 1973).
5. E. A. Boudreaux and L. N. Mulay (Eds.), *Theory and Applications of Molecular Paramagnetism* (Wiley, New York, 1976).
6. M. Gerloch, *Magnetism and Ligand Field Analysis* (Cambridge University Press, 1983).
7. R. L. Carlin and A. J. van Duyneveldt, *Magnetic Properties of Transition Metal Compounds* (Springer-Verlag, Berlin, 1977); R. L. Carlin, *Magnetochemistry* (Springer-Verlag, Berlin, 1986).
8. D. Babel, *Structure and Bonding* **3**, 1 (1967).
9. D. Babel, and A. Tressaud, *Inorg. Solid Fluorides*, (ed. P. Hagenmuller) (Academic, New York, 1985), p. 77.
10. W. Rüdorff, J. Kändler and D. Babel, *Z. Anorg. Allg. Chem.* **317**, 261 (1962).
11. W. Rüdorff, G. Lincke and D. Babel, *Z. Anorg. Allg. Chem.* **320**, 150 (1963).
12. M. Steiner, W. Krüger and D. Babel, *Solid State Commun.* **9**, 227 (1971).
13. G. Heger, R. Geller and D. Babel, *Solid State Commun.* **9**, 335 (1971).
14. F. Binder, Thesis, Tübingen, 1973.
15. W. D. Griebler, Thesis, Marburg, 1978.
16. A. Hartung, Thesis, Marburg, 1978.

17. A. Hartung and D. Babel, *J. Fluorine Chem.* **19**, 369 (1982).
18. H. Holler, J. Pebler and D. Babel, *Z. Anorg. Allg. Chem.* **522**, 189 (1985).
19. W.-D. Griebler and D. Babel, *Z. Naturforsch.* **37**, 832 (1982).
20. W. Kurtz and D. Babel, *Solid State Commun.* **48**, 277 (1983).
21. M. Witzel, Thesis, Marburg, 1985.
22. G. T. Rado and H. Suhl (Eds.), *Magnetism*, 5 Volumes (Academic, New York, 1963–1975).
23. D. H. Martin, *Magnetism in Solids* (Jliff Books, London, 1967).
24. J. Crangle, *The Magnetic Properties of Solids*. (E. Arnold, London, 1977).
25. L. J. de Jongh and A. R. Miedema, Experiments on Simple Magnetic Model Systems, *Adv. Phys.* **23**, 1–260 (1974).
26. R. D. Willett, D. Gatteschi and D. Kahn (Eds.), *Magneto-Structural Correlations in Exchange Coupled Systems*, NATO ASI Series C, Vol. 140 (Reidel, Dordrecht, 1985).
27. A. Tressaud and J. M. Dance, *Adv. Inorg. Chem. Radiochem.* **20**, 133 (1977); *Structure and Bonding* **52**, 87 (1982); *Inorg. Solid Fluorides*, ed. P. Hagenmuller (Academic, New York, 1985), p. 371.
28. H. A. Kramers, *Physica* **1**, 182 (1934).
29. P. W. Anderson, *Phys. Rev.* **79**, 350 (1950), *ibid.* **115**, 2 (1959); *Solid State Phys.* **14**, 99 (1963).
30. J. B. Goodenough, *J. Phys. Chem. Solids* **6**, 287 (1958).
31. J. Kanamori, *J. Phys. Chem. Solids* **10**, 87 (1959).
32. W. Massa, unpublished.
33. J. M. Dance, J. Mur, J. Darriet, P. Hagenmuller, W. Massa, S. Kummer and D. Babel, *J. Solid State Chem.* (in press).
34. M. Vlasse, G. Matejka, A. Tressaud and B. M. Wanklyn, *Acta Crystallogr. B* **33**, 3377 (1977).
35. A. Okazaki and Y. Suemune, *J. Phys. Soc. Japan* **16**, 176 (1961).
36. D. Babel, *Z. Anorg. Allg. Chem.* **336**, 200 (1965).
37. E. König, *Landolt-Börnstein Tables*, New Series II/2, 2-343. (Springer-Verlag, Berlin, 1966).
38. W. Massa and J. Pebler, *J. Solid State Chem.* (to be published).
39. M. Steiner, J. Villain and C. G. Windsor, *Adv. Phys.* **25**, 87 (1976).
40. R. E. Schmidt, Thesis, Marburg, 1985.
41. J. E. Weidenborner and A. L. Bednowitz, *Acta Crystallogr. B* **26**, 1464 (1970).
42. D. Babel, *Z. Anorg. Allg. Chem.* **369**, 117 (1969).
43. K. Knox and S. Geller, *Phys. Rev.* **110**, 771 (1958).
44. K. Lee, A. M. Portis and G. L. Witt, *Phys. Rev.* **132**, 144 (1963).
45. V. Scatturin, L. Corliss, N. Elliott and J. Hastings, *Acta Crystallogr.* **14**, 19 (1958).
46. D. Babel, G. Pausewang and W. Viebahn, *Z. Naturforsch.* **22b**, 1219 (1967).
47. D. Babel, *Z. Anorg. Allg. Chem.* **387**, 161 (1972).
48. A. Hartung, W. Verscharen, F. Binder and D. Babel, *Z. Anorg. Allg. Chem.* **456**, 106 (1979).
49. R. D. Shannon, *Acta Crystallogr. A* **32**, 751 (1976).
50. D. Babel and F. Binder, *Z. Anorg. Allg. Chem.* **505**, 153 (1983).
51. H. Holler, D. Babel, M. Samouel and A. de Kozak, *Rev. Chim. Miner.* **21**, 358 (1984).
52. E. Herdtweck and D. Babel, *Z. Anorg. Allg. Chem.* **474**, 113 (1981).
53. E. O. Wollan and W. C. Koehler, *Phys. Rev.* **100**, 545 (1955).
54. E. O. Wollan, H. R. Child, W. C. Koehler and M. K. Wilkinson, *Phys. Rev.* **112**, 1132 (1958).

55. G. Toulouse, *Commun. Phys.* **2**, 115 (1977).
56. G. Ferey, M. Leblanc, R. de Pape and J. Pannetier, *Inorg. Solid Fluorides*, ed. P. Hagenmuller (Academic, New York, 1985), p. 395.
57. W. Kurtz, *Solid State Commun.* **42**, 871 (1982).
58. C. Pappa, J. Hammann and C. Jacoboni, *J. Phys.* **46**, 637 (1985).
59. L. Bevaart, P. M. H. L. Tegelaar, A. J. van Duyneveldt and M. Steiner, *Phys. Rev. B* **26**, 6150 (1982).
60. D. Babel, F. Binder and G. Pausewang, *Z. Naturforsch.* **28b**, 213 (1973).
61. R. M. Bozorth, H. J. Williams and D. E. Walsh, *Phys. Rev.* **103**, 572 (1956).
62. F. Hulliger, M. Landolt and H. Vetsch, *J. Solid State Chem.* **18**, 283 (1976).
63. R. Klenze, B. Kanellakopulos, G. Trageser, and H. H. Eysel, *J. Chem. Phys.* **72**, 5819 (1980).
64. J. F. Keggin and F. D. Miles, *Nature* **137**, 577 (1936).
65. M. Witzel and D. Babel, *Z. Naturforsch.* **40b**, 1344 (1985).
66. H. Henkel and D. Babel, *Z. Naturforsch.* **39b**, 880 (1984).
67. D. Babel, R. Haegele, G. Pausewang and F. Wall, *Mater. Res. Bull.* **8**, 1371 (1973).
68. S. Emori, M. Inoue, M. Kishita and M. Kubo, *Inorg. Chem.* **8**, 1385 (1969).
69. F. J. Darnell and W. H. Cloud, *Colloq. Internat. C.N.R.S., Soc. Chim.* 5^e Série (1965), p. 1164.
70. M. M. Schieber, *Experimental Magnetochemistry*, Vol. VIII of Selected Topics in Solid State Physics, ed. E. P. Wohlfarth (North-Holland, Amsterdam, 1967).